Journal of Applied Geophysics, 29 (1993) 211–226
Elsevier Science Publishers B.V., Amsterdam

Two-dimensional resistivity imaging and modelling in areas of complex geology

D.H. Griffiths and R.D. Barker
School of Earth Sciences, University of Birmingham, Edgbaston, Birmingham B15 2TT, UK

(Accepted after revision September 30, 1992)

ABSTRACT

Griffiths, D.H. and Barker, R.D., 1993. Two-dimensional resistivity imaging and modelling in areas of complex geology. In: R. Cassinis, K. Helbig and G.F. Panza (Editors), Geophysical Exploration in Areas of Complex Geology, I. J. Appl. Geophys., 29: 211–226.

A system is described for the automatic measurement of electrical resistivity pseudo-sections. This comprises a linear array of up to 32 electrodes connected through a multicore cable to a computer controlled switching module and a resistivity meter. The processing of the measured sections to produce two-dimensional true resistivity images of the subsurface is briefly described. Some account is given of the capabilities and limitations of the technique. This is illustrated by a series of computed constant separation traverses for models of simple subsurface structures. Examples of processed images derived from sections measured in areas of relatively complex geology follow, a comparison being made of the interpretations obtained using an automatic imaging method and a manual iterative approach. It is concluded that with the equipment and software so far developed, in areas of modest subsurface geological complexity where some control is available and where the structures are essentially two-dimensional, then good approximations to the true geoelectric sections can be obtained down to depths of between 100 and 200 m.

Introduction

Electrical imaging or electrical tomography is a survey technique recently developed for the investigation of areas of complex geology where the use of resistivity sounding and other techniques is unsuitable. There is increasing interest, particularly in mineral, groundwater and engineering investigations, in imaging the distribution of the electrical properties in the subsurface. However, in the medical field also, electrical imaging techniques have been developed for investigation of the human torso (Barber and Seagar, 1987). Medical success has been obtained with the use of electrodes which surround or partially surround the area to be imaged. Barber and Brown (1984) reviewed the use of arrays of electrodes surrounding the body and simple backprojection techniques to produce approximate cross-sectional images of the body. They refer to these techniques as "applied potential tomography".

In geological applications, tomographic surveys normally employ arrays of electrodes on the surface of the ground for data collection. The survey technique involves measuring a series of constant separation traverses with the electrode separation being increased with each successive traverse. Because increasing the separation leads to information from greater depth, the measured apparent resistivities may be plotted as a contoured section, which reflects qualitatively the spatial variation in resistivity in the vertical cross-section. Length of

profile, depth penetration and resolution required determine the unit electrode spacing which can be anywhere from 1 m to 50 m or more.

The contoured data may be modelled using a two-dimensional (2-D) finite element or finite difference algorithm (Dey and Morrison, 1979) and commercially available software now enables quite complex modelling to be carried out. Alternatively the data can be inverted automatically to provide an image of true resistivity. It is the automatic nature of this process of interpretation which enables it to be termed "imaging". No a priori information on the distribution of resistivity is involved and the resulting image is free from interpreter bias (West and Bailey, 1988).

Our own work on electrical imaging has centred around the development of computer controlled data collection and also automatic data inversion. In the following pages we describe the instrumentation and field systems we have developed, the modelling methods, automatic inversion techniques and finally some examples of their use.

Field systems

For imaging to depths of less than 30 m it is convenient to use electrode spacings of 10 m or less and for this purpose a single multicore cable to which all the electrodes are connected at takeouts moulded on at predetermined positions can be used. The cables are connected to a switching module in a specially designed earth resistivity meter which is controlled by a computer through an RS232 port.

The control software is designed to carry out a series of constant separation traverses with increasing electrode spacing at each traverse. Alternatively a "roll-along" technique may be used (Fig. 1). Here, measurement commences at one end of the line using electrodes 1, 2, 3 and 4. The spacing is then doubled without moving on, the active electrodes being 1, 3, 5 and 7. At each measurement, spacing is increased by one unit until the maximum spacing is reached ($n=8$ is possible for a 25 electrode array), after which the sequence is repeated starting with electrodes 2, 3, 4 and 5. Normally measurements are made for levels

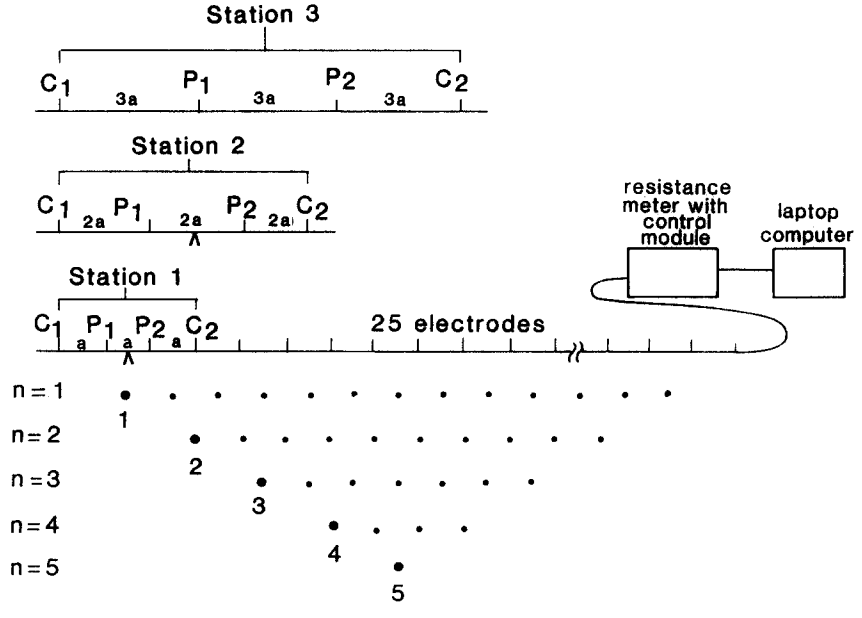

Fig. 1. The measurement sequence for building up a pseudo-section.

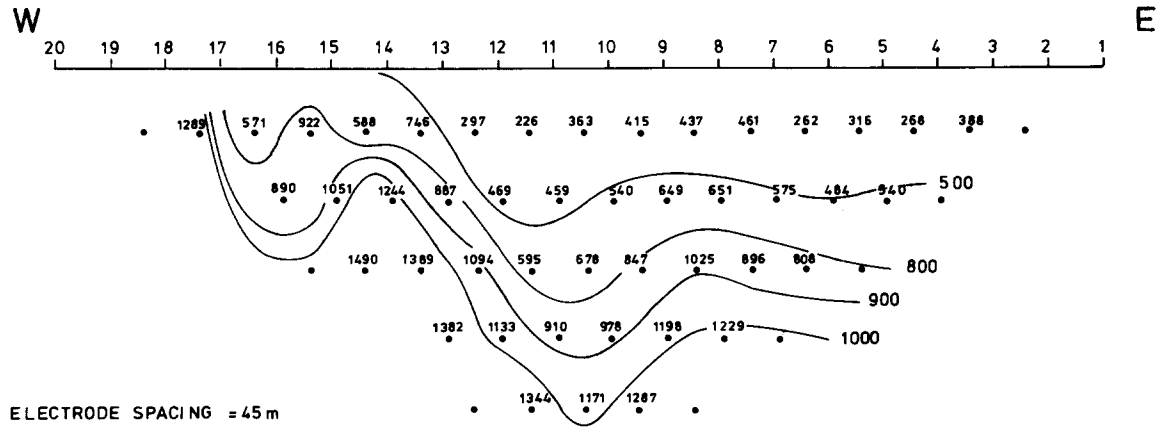

Fig. 2. An example of a Wenner pseudo-section.

$n=1$ to $n=6$ for the first 6 stations after which the electrodes 1 to 6 are picked up and moved to the front of the line, the cable shifted forward and reconnected. This process is repeated until the traverse is complete.

A common method of presenting profiling data made at several spacings is as a pseudo-section, a technique introduced by Hallof (1957) for plotting data measured with the dipole–dipole electrode arrangement. However, so far, for imaging purposes, we have found the Wenner electrode array the most satisfactory. Wenner pseudo-sections have some advantages over dipole–dipole pseudo-sections, the most important of which is that Wenner profiling data are less affected by near-surface resistivity variations which on dipole–dipole pseudo-sections can cause strong distortions of the contours.

The construction of a pseudo-section is achieved by plotting the measured apparent resistivity on a section below the centre point of the array at a depth which is a fraction of the electrode spacing, a (Fig. 1). Sections which most closely approximate a true depth scale are best obtained by plotting depth equal to half the inter-electrode spacing, a (Edwards, 1977). The plotted values are contoured to provide the pseudo-section, an example of which is shown in Fig. 2.

For imaging to depths of more than 30 m and hence with electrode spacings of more than 10 m, the use of a single multicore cable becomes difficult and it is more practicable to house the relays at each electrode. A system developed by us (Griffiths and Turnbull, 1985; Griffiths et al., 1990) at the University of Birmingham and known as the Microprocessor-controlled Resistivity Traversing (MRT) System, uses 25 equally spaced electrodes (although up to 32 can be used), each linked to the next by 50 m of light, 7-core, reel-mounted cable. Addressa-

[1]CAMPUS Geophysical Instruments Ltd

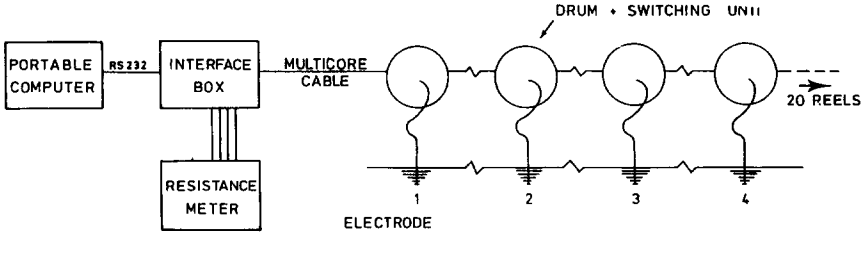

Fig. 3. Layout of the MRT system control units.

ble electronic switching units, which are mounted in the reel hubs and powered by small rechargeable batteries, enable any four electrodes to be connected simultaneously to the resistivity meter. The layout of the equipment is shown in Fig. 3. Any IBM compatible PC can be used to control the switching and the system can be used with any resistivity meter. Our version, however, employs the Campus GEOPULSE [1] meter. Using this system, measurement of the full pseudo-section is automatic and the data are stored on a laptop computer. Using a "roll-on" sequence of measurements, as shown in Fig. 1, continuous profiling is possible, requiring a change of operator position once every 50 electrode positions.

A number of considerations govern field layout and the quality of data collected. The first consideration is the depth of investigation required, for this fixes the maximum electrode separation. For a Wenner spread a rough guide is to make this twice the depth down to which information is required (Edwards, 1977). For the standard MRT array of 25 electrodes set out at the maximum inter-electrode spacing, a, of 50 m, the maximum possible measurement separation is 400 m, giving a depth of investigation of around 200 m. This sets a limit to both the horizontal resolution and the near-surface vertical resolution.

Interpretation

Provided the subsurface structure is essentially two-dimensional and the measured profile is perpendicular to the strike direction, the spatial positions of the apparent resistivity values of the pseudo-section are in many instances qualitatively related to the distribution of true resistivity in the cross-section of the ground below the profile. The pseudo-section can therefore be considered to be a very smoothed image. Processing the data, i.e. "interpreting" it, is therefore a matter of sharpening up and correctly scaling the apparent resistivity image. Two approaches to this are possible.

A manual interactive approach is to use semi-quantitative methods to create an initial model and then to calculate the apparent resistivity pseudo-section from this using a finite difference or finite element algorithm. After comparing the computed section with the field data, appropriate adjustments are made to the model parameters and a further computation made. Success tends to depend on the quality of the initial model but a satisfactory fit to the field data can be reached after 7–10 iterations especially where the structure is of limited complexity.

An alternative approach is to use an automatic iterative method (Barker, 1992) which considerably sharpens up the image, places the structures at approximately their correct depth, and provides acceptable estimates of their true resistivities. However, both lateral and vertical resistivity changes, even if in reality these are sharp discontinuities, show as gradational changes in the construction of the image. This only presents difficulties in certain instances as many geological boundaries are in fact gradual. The process uses a finite difference algorithm (Dey and Morrison, 1979) at each step to produce an apparent resistivity section, compares this with the field data and modifies the model until an acceptable fit between field and computed pseudo-sections is achieved. The process can achieve a solution within 5 iterations and with good data the convergence is very stable. Where the data are noisy it may be necessary to apply some smoothing.

As is the case when carrying out resistivity sounding, the interpretation of two-dimensional data is subject to the limitations of equivalence and suppression. As discussed below the decrease in resolution with depth also

imposes considerable constraint on the accuracy of interpretation. This is particularly so where no additional information, such as that provided by a borehole, is available. Furthermore, because two-dimensional algorithms are being used for interpretation, the subsurface structure must also approximate to two-dimensionality in a direction roughly perpendicular to the measured profile. In areas of complex geology this is likely to be only roughly true at best.

Some illustrative models

Though ultimately the test of a new technique is its success in the field, we can learn a great deal about its capabilities and limitations from two-dimensional computer modelling. What we are particularly interested in are detectability and resolution under varying conditions. Modelling a wide range of situations is a considerable task and here we have only selected a few simple but important models to illustrate what can be mapped over somewhat less than simple geology. Previous work in this context carried out by Olayinka (1988) is also relevant.

Setting aside for the moment the effects of "noise" i.e. the effects of near-surface local variations in resistivity that in themselves may place a limit on the detectability and resolution of deeper structures, what are the important variables? They are, of course, structural dimensions relative to depth and resistivity contrast. However, not only must a volume of rock be sufficiently large and show a large enough contrast with its surroundings to produce a recognisable anomaly but it must be separated from adjacent bodies by a sufficient distance for it to be resolvable. These we might call the minimum conditions. Such factors as, for example, lateral variation within a body could be a further complication. More important, because here we are measuring only profiles, in carrying out quantitative interpretation we are assuming structures to be not only two-dimensional but extended in the horizontal direction perpendicular to the profile. This can be an unrealistic assumption but in practice often not as serious as might be thought.

Below we consider a few simple two-dimensional structures, firstly a filled fracture zone in crystalline basement with a thin overburden of unconsolidated material of low resistivity and, secondly, topography on the basement in the form of a rectangular upfaulted block. Finally we examine a few simple fault models in a sedimentary sequence. These few examples are sufficient to give us a useful insight into what can and what cannot be done in the way of interpretation of two-dimensional array data.

Figure 4a shows a series of profiles obtained with an expanding Wenner electrode arrange-

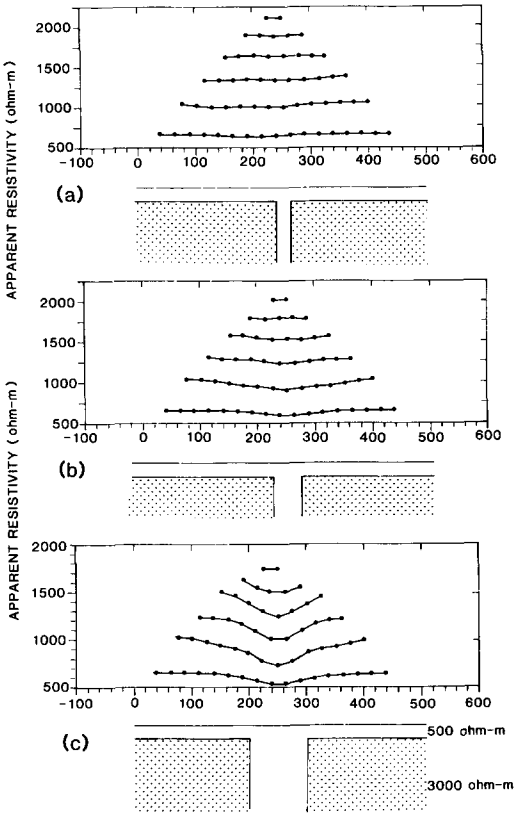

Fig. 4. Computed constant separation profiles with an expanding Wenner system ($a=25$ m) across an infilled vertical fissure under 25 m of overburden width. (a) 25 m; (b) 50 m; (c) 100 m; $\rho_1=500$ ohm·m, $\rho_2=3000$ ohm·m.

ment over a 25 m wide infilled fissure in basement under 25 m of overburden. The resistivity contrast is high but the fissure is hardly detectable. A width/depth ratio of 1.0 is thus the limit. As Fig. 4b shows, a width/depth ratio of 2.0 even at high contrast does not produce a large anomaly. We have to increase the width to 100 m to produce an anomaly of considerable size (Fig. 4c). Note that the anomaly amplitude does not change if we scale up the model, provided the width/depth ratio is not changed. Interestingly, for a given model, it is not necessarily the highest contrast that produces the maximum amplitude anomaly. With very low top layer resistivities much of the current is confined to the overburden and the fissure would have less effect.

Now consider Fig. 5a, the upfaulted basement block, here 25 m high and 25 m wide and with a depth to top of 50 m. The contrast between basement and overburden is $k=0.93$. The anomaly at $n=3$ is about 14% of the background value, probably below the limit of detection in the field where local near-surface changes are often of comparable magnitude.

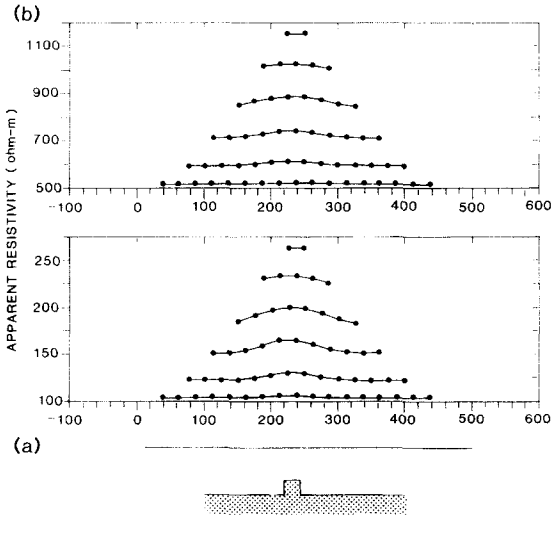

Fig. 5. Computed constant separation profiles with an expanding Wenner system ($a=25$ m) across a square upfaulted basement block 25 m wide and 25 m high with depth to top 50 m. (a) $\rho_1=100$ ohm·m, $\rho_2=3000$ ohm·m. (b) $\rho_1=500$ ohm·m, $\rho_2=3000$ ohm·m.

Increasing the overburden resistivity from 100 ohm·m to 500 ohm·m reduces the anomaly to 5% (Fig. 5b).

Finally we briefly discuss three fault models. Figure 6a is a two-layer earth in which a fault downthrows the horizontal boundary at 20 by 10 m. The resistivity contrast is $k=0.5$. The anomaly produced is very small, probably below the level of detection in the field. If we raise the boundary by 10 m without changing the fault throw the anomaly produced is well above background (Fig. 6b). In the first case $t/d=0.5$, where d is depth on the upthrow side and t is the fault displacement. In the second, t equals d. Provided the contrast is kept constant scaling up depth and throw proportionally will not affect the percentage change in the magnitude of the anomaly.

To summarise the findings so far in a very general way, we can say even when the contrast is considerable the dimensions of a structure have to be comparable with its depth for it to

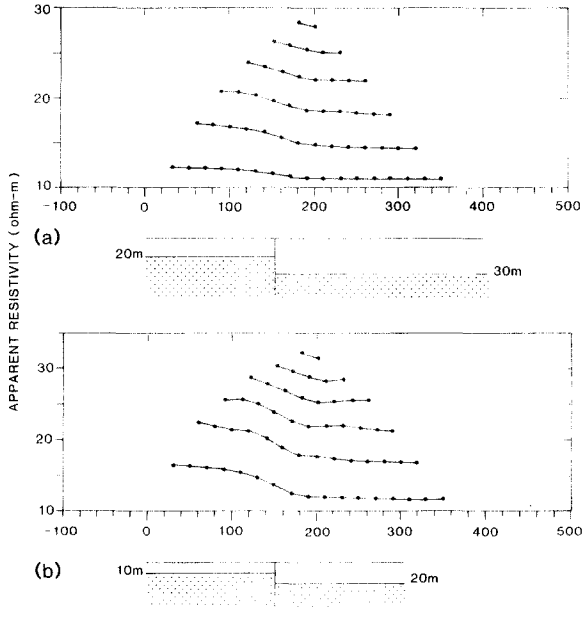

Fig. 6. Computed constant separation traverses with an expanding Wenner electrode system ($a=20$ m) over a basement step (vertical fault). Overburden $\rho_1=10$ ohm·m, basement $\rho_2=30$ ohm·m. (a) Downthrow from 20 to 30 m. (b) Downthrow from 10 to 20 m.

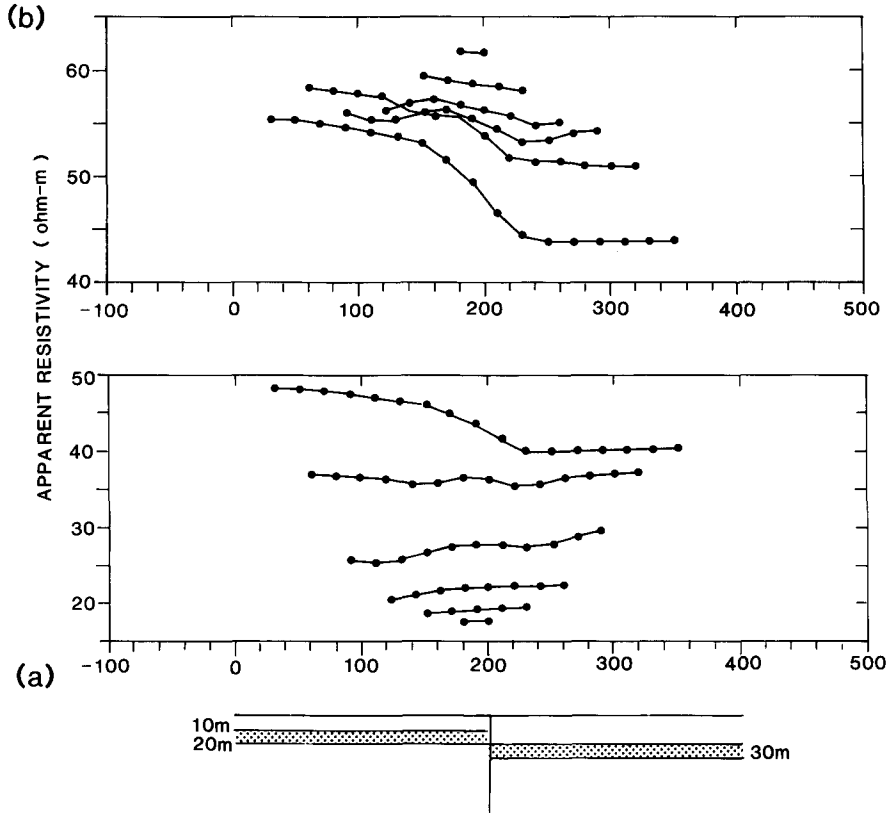

Fig. 7. Computed constant separation traverses with an expanding Wenner electrode system (a=20 m) across a down-faulted sequence of 3 layers. Fault throw 10 m. (a) Top layer 10 m, 40 ohm·m, middle layer 10 m, 100 ohm·m, basement 40 ohm·m. (b) The same as (a) but basement now 12 ohm·m.

produce a marked effect on resistivity measurements.

So far the structures considered have been very simple indeed. A measure of complexity is added by introducing a third layer, as shown in Fig. 7a. The 10 m thick 100 ohm·m layer separates upper and lower strata of 40 ohm·m. The fault throw is again 10 m. The anomaly is clearly defined but no more than about 15% of the background. From a careful study of the pseudo-section it would be possible to draw a qualitatively correct diagram of the structure and inversion would produce an approximately correct interpretation. However, merely by changing the resistivity of the lower layer to 12 ohm·m, that is, by creating a faulted three-layer structure, as shown in Fig. 7b, the resulting anomaly much less obviously reflects the structure.

From the simple examples discussed above, some of the limitations of two-dimensional resistivity surveying become obvious.

Field examples

We discuss below a few representative images which illustrate what can be achieved with the technique.

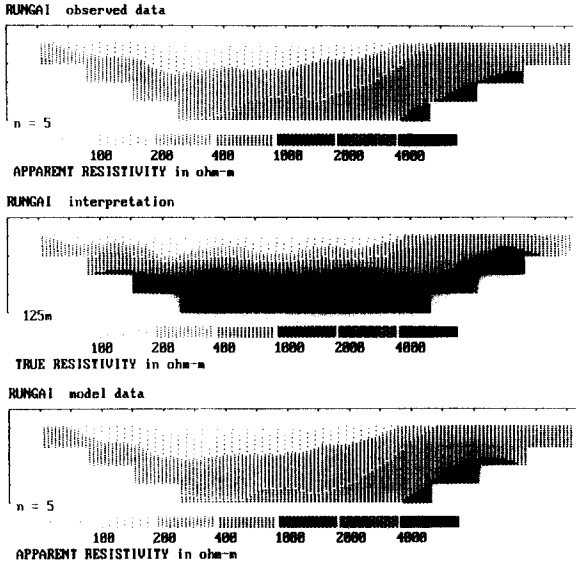

Fig. 8. Apparent resistivity and true resistivity images of a section of weathered crystalline basement at Rungai, Zimbabwe. The apparent resistivity image computed from the model is given for comparison.

Rungai, Zimbabwe

The Wenner section shown in Fig. 8 was measured during a hydrogeological investigation over deeply weathered crystalline basement rock. It runs W–E just south of outcrops near the ends of the 1 km long line. A 50 m electrode spacing was used. The upper image is a plot of the measured apparent resistivity pseudo-section down to $n=5$. Examination of the section indicates the presence of a shallow basin of low-resistivity weathered rock with the basement rising to the near-surface at the two ends of the line. The lower image is the true resistivity plot obtained after 6 iterations of the inversion program. This shows a thin, quite low-resistivity surface layer, probably clay rich in character, below which the resistivity rises steadily to values of 2000 ohm·m or more at a depth of around 100 m. In this environment a gradual transition from fully weathered low-resistivity material to high-resistivity unfractured fresh rock is quite possible. If this is the case the choice of depth to bedrock at any point is somewhat arbitrary. However, as already explained, even sharply contrasting boundaries appear transitional on a processed image, though considerably sharper than on the unprocessed image, so the nature of the boundary is left in doubt. Nevertheless, from experience we can say that rock with a resistivity of 1000 ohm·m can certainly be classed as basement. The image, therefore, is of a shallow basin in the crystalline basement overlain by lower- but intermediate-resistivity material, with a low-resistivity surface layer. The intermediate material is probably sandy and water bearing, the near-surface possibly clay rich.

We now turn to an interpretation obtained by repeated forward modelling with manual adjustment of the model at each stage until convergence is achieved. The interpretation, as one would expect, is qualitatively similar but there are differences. The reasons for this are equivalence and the difficulty of achieving a close fit, particularly where no other information is available on depths or resistivities and where conditions are such that the measurements themselves provide little top layer information. Figure 9 shows a model which is a fair fit to the data and which uses realistic values for the layering. The choice was guided by interpreting vertical columns of data from the pseudo-section as soundings, interpolating where necessary. An example is given in Fig. 10. Note that, as a consequence of the high resistivity of the basement and its relatively shallow depth, all points but the first at an expansion of 50 m lie on almost a straight line. The curve has to be interpreted as a two-layer or at the most a three-layer curve and there is considerable ambiguity about the fit. Here there is a sharply defined boundary between low-resistivity weathered material and high-resistivity fresh crystalline basement. Furthermore the model indicates that the fresh rock lies closer to the surface than is suggested by the model produced by automatic inversion. In the absence of independent information such as

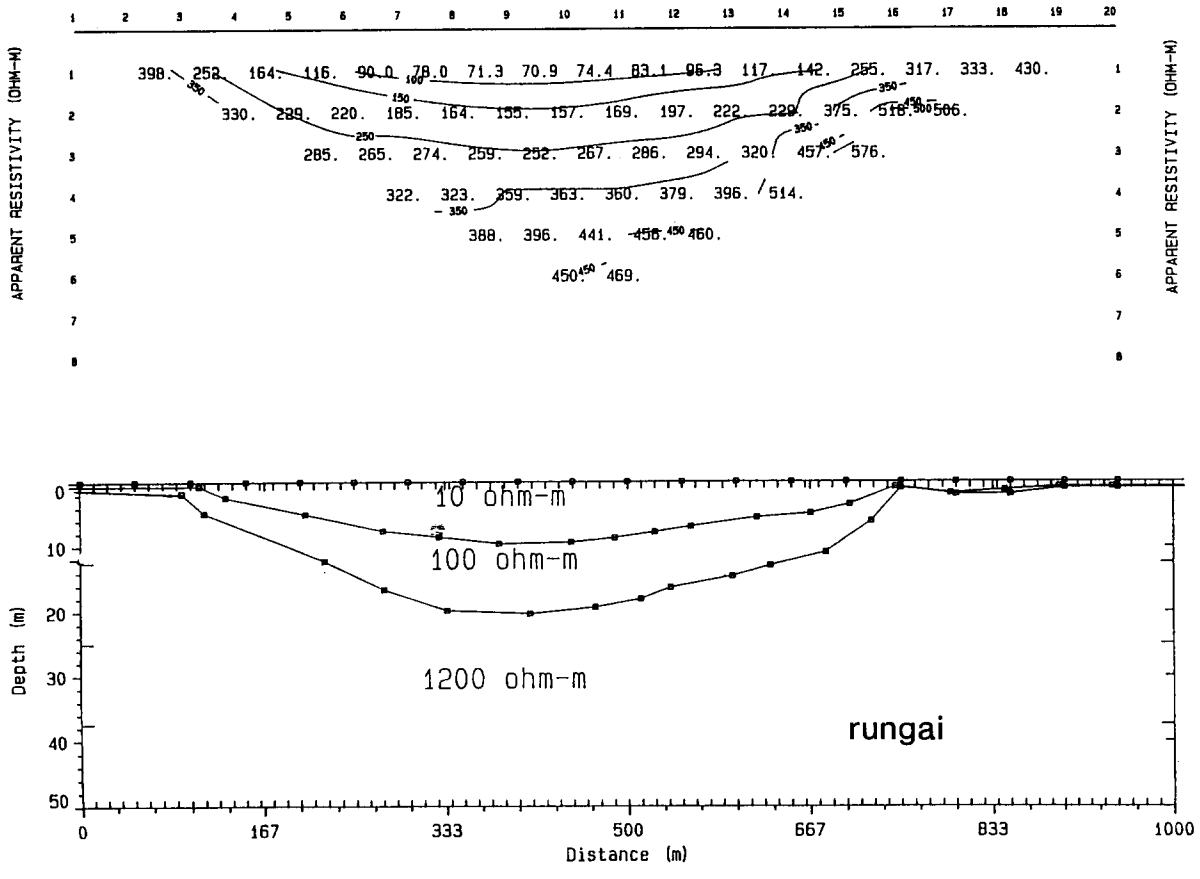

Fig. 9. Two-dimensional model obtained by forward modelling to fit the data from Rungai.

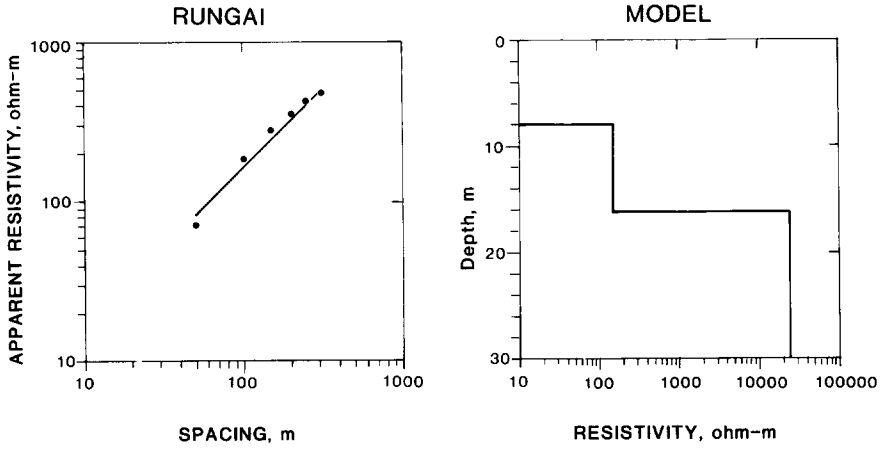

Fig. 10. Interpreted "pseudo-sounding" using apparent resistivity data from the Rungai profile.

borehole data, neither interpretation can be dismissed, though if a choice has to be made, closeness of fit between the measured apparent resistivities and the apparent resistivities computed from the model has to be considered.

Mhativa, Zimbabwe

This profile was also obtained in the course of a hydrogeological survey in Zimbabwe and was measured across a shallow valley which previous data (Smith and Raines, 1988) had suggested was the site of a deeply weathered and thus low-resistivity fracture zone in the crystalline bedrock. Elsewhere the weathered layer was known to be no more than a few metres thick at the most. Thus, unlike conditions at Rungai, some constraint was available. To obtain good top layer information it would have been necessary to reduce the electrode separation to 10 m but this would have unduly limited both depth of investigation and profile length. A compromise of 20 m was therefore adopted, this giving adequate depth of investigation and an acceptable lateral resolution, the latter being important as the main aim of the profile was to delineate the fissure zone.

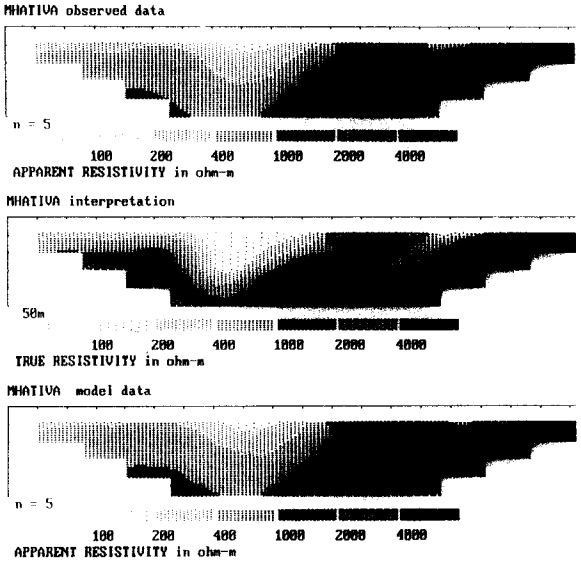

Fig. 11. Apparent resistivity and true resistivity images from a fissured basement section at Mhativa with apparent resistivity section computed from the model image for comparison.

The apparent resistivity measurements are shown in the upper section of Fig. 11. They show a deep steep sided zone of low resistivity, some 40 m wide, in the centre of the section, with the basement rising to shallow depths at the ends of the profile. Following inversion these features are enhanced. The true resistivity plot shows the low-resistivity weathered zone extending to at least 30 m. A second interesting feature is the relatively gently dipping low-resistivity, presumably weathered, zone in the basement seen towards the right hand end of the section. It is useful to compare the interpreted section with a simple parallel sided vertical fissure zone model such as that of Fig. 4c. There is a considerable similarity.

Staffordshire, England

Figure 12 shows the apparent resistivity pseudo-section and interpretation of a 3 km long W–E profile measured over Triassic and Carboniferous sediments on the edge of the Staffordshire basin. The strata dip gently westwards and are strongly faulted in a more or less N–S-direction. A nearby profile gave a very similar pseudo-section, indicating that the subsurface structure is two-dimensional in a direction perpendicular to the measured line. The geological succession in the area was known from boreholes and is shown in Fig. 12. Data from a few soundings were also available. There is good contrast between the low-resistivity Mercia Mudstone and the Cannock Formation, the Bromsgrove Formation being of intermediate resistivity

An electrode separation of 50 m was used for the MRT survey, providing a maximum electrode separation of 300 m and thus a nominal depth of investigation of 150 m. Inspection of the contour pattern of the pseudo-section and the lateral changes in resistivity indicated the

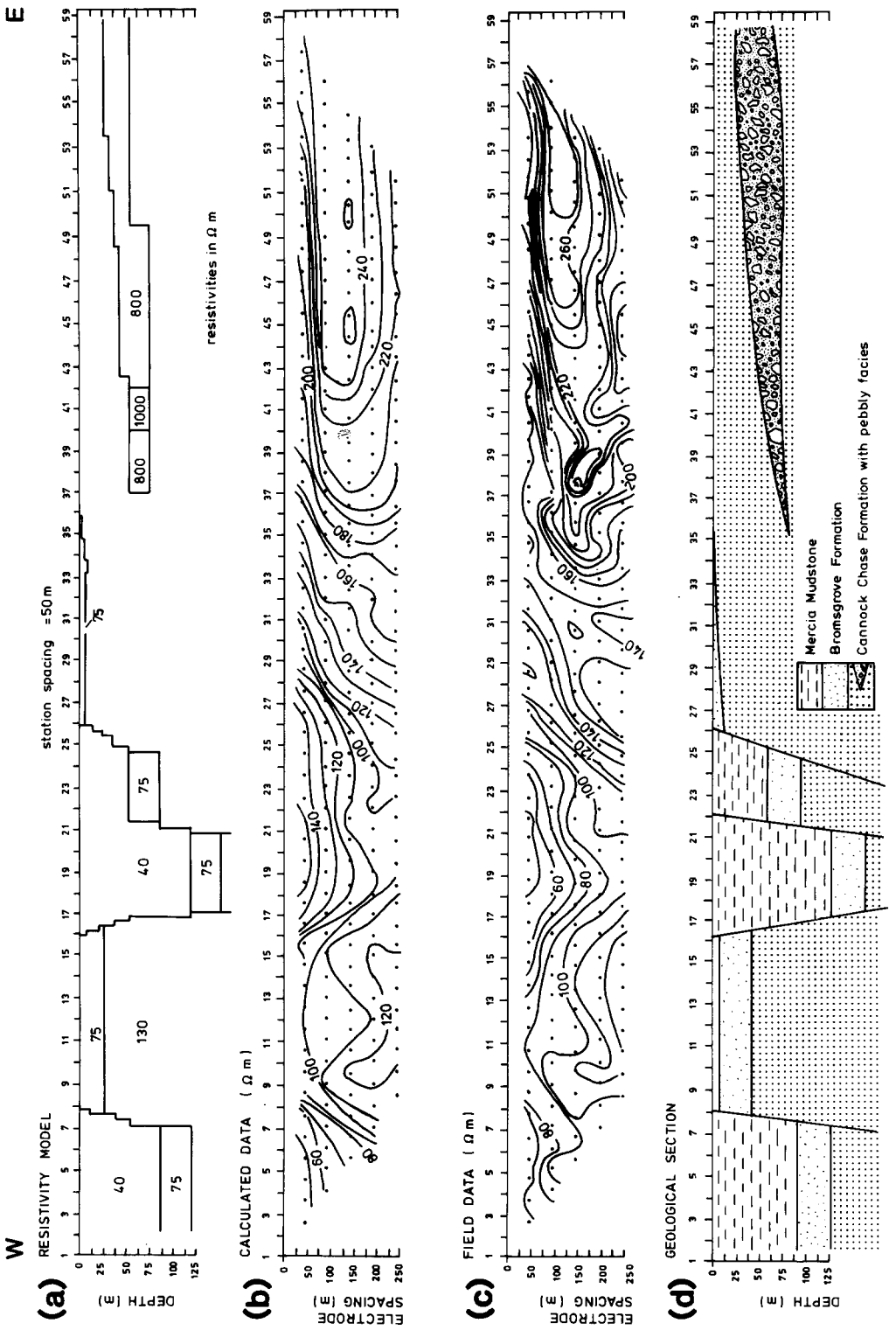

Fig. 12. Interpretation of a faulted Triassic sequence in Staffordshire. (a) Two-dimensional model. (b) Computed apparent resistivity pseudo-section. (c) Field data. (d) Geological interpretation based on (a) and additional information (after Griffiths et al., 1990).

Mudstone and the lower high-resistivity layer being due to the combined effects of the Bromsgrove and Cannock Formations. The very high resistivities in the Cannock beds in the east were thought to be due to a pebbly facies. Using borehole and available resistivity data, the model was then refined by separating the lower layer into two parts, the Bromsgrove Formation of intermediate resistivity and the higher-resistivity Cannock Formation beneath. After some adjustment an acceptable model was obtained showing an *RMS* error be-

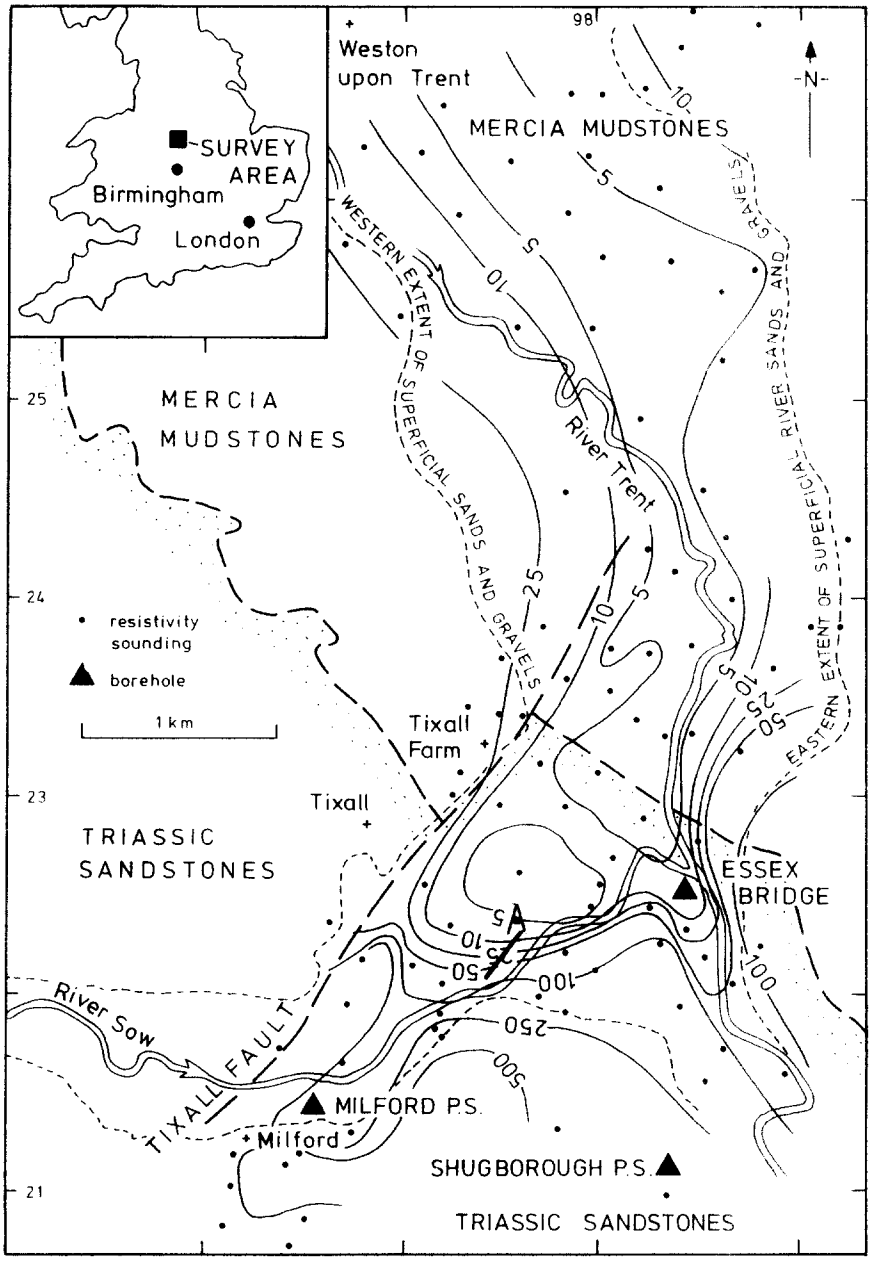

Fig. 13. Map of the Shugborough area Staffordshire showing contours of bedrock resistivity in ohm·m, and the position of MRT (line *A*).

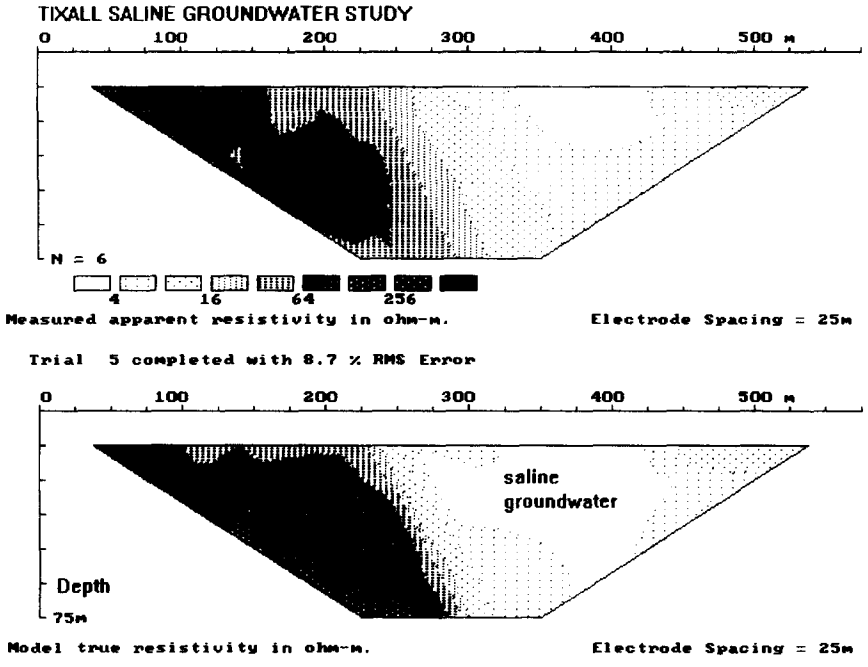

Fig. 14. Measured apparent resistivity image showing the fresh water–saline water interface at Shugborough and true resistivity model image.

tween the observed and calculated apparent resistivities of just less than 3%.

Saline groundwater, Staffordshire

Our final example presents the results of electrically imaging the strong resistivity contrast which can occur across the junction between fresh and saline groundwater.

The presence of an area of saline groundwater to the west of Stafford has been known for many years. Three boreholes had been sunk in the Sherwood Sandstone in the Shugborough Park area east of Stafford (Fig. 13). Two of these, at Milford and Shugborough pumping stations, supply fresh water while that at Essex Bridge yields highly saline water (15,000–20,000 mg/l Cl^-). The source of the high salinity is thought to be saliferous beds in the Mercia Mudstones. The Triassic sandstones and mudstones in this area are covered by sediments of the River Trent and it is possible that groundwater moving through the sediments is dissolving the salt from the underlying formations and carrying it south into the Triassic sandstones. Clearly there was a need to identify the extent of the saline groundwater in the area and at the same time to study the subdrift geology.

To locate the body of saline groundwater, 58 resistivity soundings were measured in 1978 (Barker, 1980) and further measurements made in 1991. The presence of the high-salinity groundwater was clearly recognised from the low resistivities obtained from many of the soundings measured between Essex Bridge and Tixall. Bedrock resistivities lower than 5 ohm·m were recorded in many places. The extent of the saline groundwater may be seen on the map of bedrock resistivity shown in Fig. 13 where the area of strongly saline groundwater is approximately defined by the 100 ohm·m contour. Saline groundwater is seen to occur in the whole region between Tixall Farm and Essex Bridge.

In order to examine the form of the junction between the fresh and saline groundwater an electrical image was measured across the front

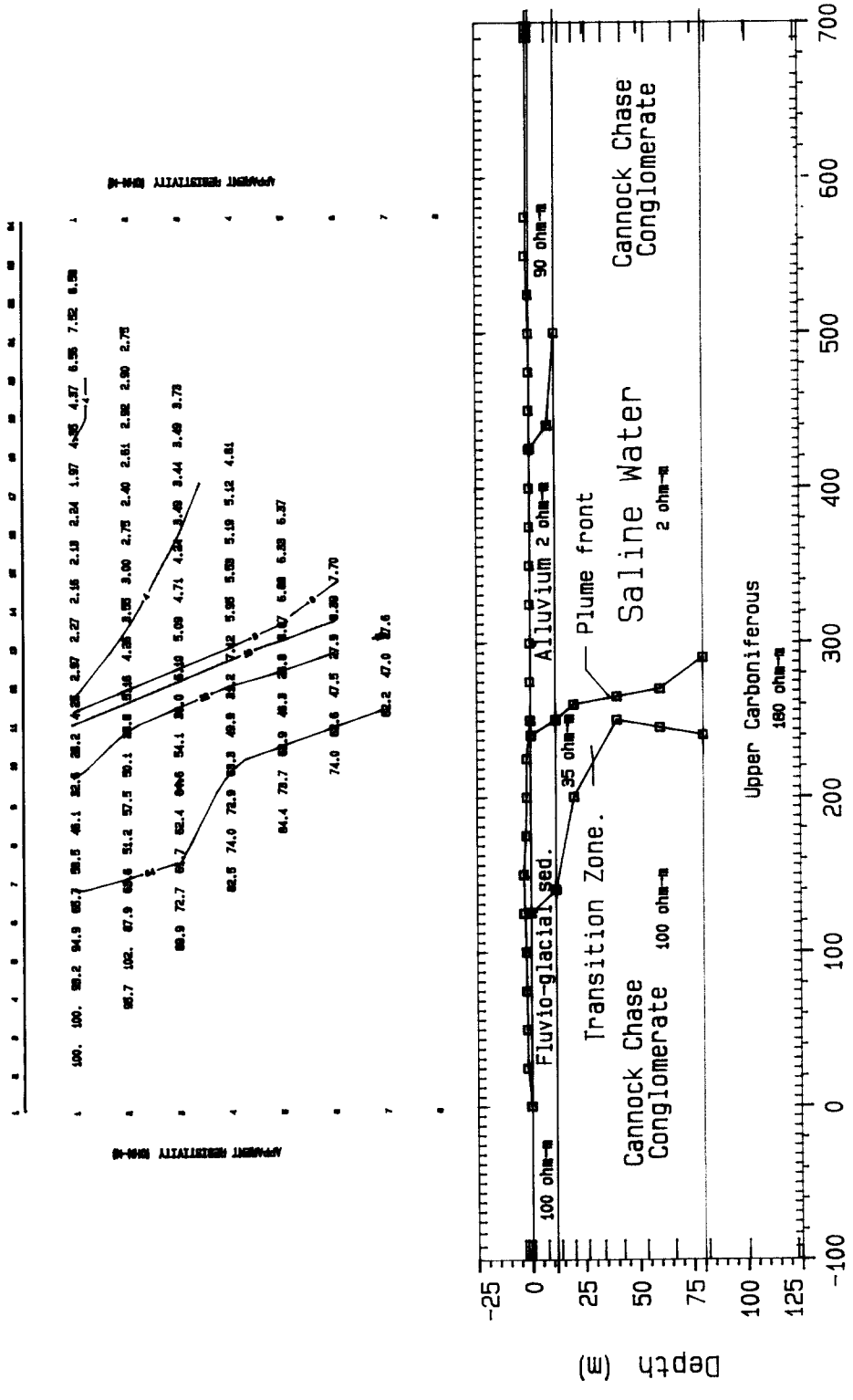

Fig. 15. Two-dimensional model of the fresh water–saline water interface at Shugborough and the calculated pseudo-section.

at one of its sharpest points (*A* in Fig. 13). A Campus GEOPULSE and an MRT system with an electrode spacing of 25 m and multiples of unit electrode spacing from $n=1$ to $n=6$ were employed. The data were automatically processed to produce the electrical image shown in Fig. 14. Here, the change in apparent resistivity, which in the measured pseudo-section is shown to be gradual, proves to be quite sharp in the processed image. The thickness of the transition zone could in fact be sharper than the electrode spacing which in this example sets a reasonable limit to the resolution of the technique.

The measured pseudo-section was also modelled using RESIXIP2D, a finite element program from INTERPEX Inc. The results of this modelling, annotated with the expected geology, are shown in Fig. 15.

Discussion and conclusions

We have shown that with the available array of 25 or so electrodes set out at their maximum separation of 50 m and with computer software we can electrically image the ground down to around 200 m. Virtually continuous profiling is practical. Where the depth of investigation is less, the electrodes of the array can be more closely spaced and both vertical and horizontal resolution are consequently improved, though local near-surface resistivity variation is necessarily averaged because practical considerations set a lower limit to electrode spacing. There are no fundamental reasons preventing the use of arrays with several times as many electrodes as we have used. This would greatly improve near-surface information. However, design and weight considerations apart, laying out the array and measuring would be a very slow process. Where upper layers are thick and reasonably consistent there is no serious problem. Even so, in all circumstances borehole, sounding, electromagnetic or other data taken on or close to the section are valuable in enabling limits to be set to interpreted depths and resistivities.

Detectability and resolution both decrease with depth, setting limits to the degree of geological complexity that can be modelled. Nevertheless, despite the limitations outlined and the attendant problems of equivalence (and indeed suppression) in many circumstances the technique provides an approximately true geoelectric cross-section of the ground beneath the profile. Given some additional information relating local lithology to resistivity the electrical image can be converted to a geological section.

The application of the technique lies particularly in areas where lateral variation or geological structure render vertical electrical sounding inapplicable and where it is vital to have a continuous section.

So far the investigations have been carried out using the Wenner array. This is in general a satisfactory configuration. It has the advantage that unprocessed images are qualitatively related in form and resistivity to the true subsurface distribution of resistivity. Not only does this enable qualitative interpretation of the unprocessed image to be carried out but more accurate images are produced than can easily be obtained with some other configurations. Its resolution and depth of investigation are reasonable, it provides a strong signal and it lends itself easily to use with an equally spaced array.

Recent improvements in our technique have greatly increased the rate of data acquisition and automatic inversion very quickly provides satisfactory images from the field data. On easy ground a party of three can now cover 1.5 to 2 km of profile down to 150 m in a day. The strength of the method lies in the continuous cover obtained and the quantitative nature of the processed image. As demonstrated it has applications in hydrogeology in basement areas and to mapping in strongly faulted areas. It can be used to map rock quality for quarrying purposes and where tunnelling. It is capable of further improvement, which will come through

the use of more closely spaced electrodes and larger spreads and as a result of improved inversion programs. Considerable work needs to be done on the possibility of using focussed arrays to improve resolution and there is a need to explore the practicability of three-dimensional surveys.

Acknowledgements

We should like to acknowledge the work of past MSc students, R. Harding and research students A.I. Olayinka and J. Turnbull, who collected some of the field data, and M.H. Loke who assisted us with computer programming.

References

Barber, D.C. and Brown, B.H., 1984. Applied potential tomography. J. Phys. E, 17: 723–733.

Barber, D.C. and Seagar, A.D., 1987. Fast reconstruction of resistance images. Clin. Phys. Physiol. Meas., 8: 47–54.

Barker, R.D., 1980. Applications of geophysics in groundwater investigations. Water Serv., 84: 489–492.

Barker, R.D., 1992. A simple algorithm for electrical imaging of the subsurface. First Break, 10: 53–62.

Dey, A. and Morrison, H.F., 1979. Resistivity modelling for arbitrary shaped two-dimensional structures. Geophys. Prospect., 27: 106–136

Edwards, L.S., 1977. A modified pseudosection for resistivity and induced polarization. Geophysics, 42: 1020–1036.

Griffiths, D.H. and Turnbull, J., 1985. A multi-electrode array for resistivity surveying. First Break, 3(7): 16–20.

Griffiths, D.H., Turnbull, J. and Olayinka, A.I., 1990. Two-dimensional resistivity mapping with a computer controlled array. First Break, 8: 121–129.

Hallof, P.G., 1957. On the interpretation of resistivity and induced polarization measurements. Thesis. MIT, Cambridge, MA (unpubl.).

Olayinka, A.I., 1988. Microprocesssor Controlled Resistivity Traversing and Its Use in Borehole Siting in Basement Areas of Nigeria. PhD Thesis. Univ. Birmingham, Birmingham (unpubl.).

Smith, I.F. and Raines, M.G., 1988. Further Geophysical Studies on the Basement Aquifer in Masvingo Province, Zimbabwe. Reg. Geophys. Res. Rep., Br. Geol. Surv. (unpubl.).

West, G.F. and Bailey, R.C., 1988. Inverse methods in geophysical exploration. In: G. Garland (Editor), Proc. Exploration '87: 3rd Decennial Int. Conf. Geophys. Geochem. Explor. Miner., Ont. Geol. Surv., Spec. Vol., 3, pp. 191–212.

Zohdy, A.A.R., 1989. A new method for the automatic interpretation of Schlumberger and Wenner sounding curves. Geophysics, 54: 245–253.